THE ASTROPHYSICAL JOURNAL, 492:79–90, 1998 January 1

X-RAY SPECTRAL SURVEY OF WGACAT QUASARS. I. SPECTRAL EVOLUTION AND LOW-ENERGY CUTOFFS

FABRIZIO FIORE,[1,2,3] MARTIN ELVIS,[1] PAOLO GIOMMI,[3] AND PAOLO PADOVANI[4]
Received 1997 April 17; accepted 1997 August 11

ABSTRACT

We have used the WGA catalog of *ROSAT* Position Sensitive Proportional Counter (PSPC) X-ray sources to study the X-ray spectrum of about 500 quasars in the redshift interval 0.1–4.1, detected with a signal-to-noise ratio better than 7. We have parameterized the PSPC spectrum in terms of two "effective energy spectral indices," α_S (0.1–0.8 keV), and α_H (0.4–2.4 keV), which allows for the different Galactic $N_{\rm H}$ along the quasars' line of sight. We have used these data to explore the questions raised by the initial PSPC high-redshift quasar studies, and in particular the occurrence of low-energy X-ray cutoffs in high-redshift radio-loud quasars. We have also studied the emission spectra of a large sample of radio-loud and radio-quiet quasars and studied their differences.

We find that low-energy X-ray cutoffs are more commonly (and perhaps exclusively) found in radio-loud quasars. Therefore, the low-energy X-ray cutoffs are physically associated with the quasars, and not with intervening systems, since those would affect radio-quiet and radio-loud equally. We suggest that photoelectric absorption is a likely origin of these cutoffs.

The number of "cutoffs" in radio-loud quasars significantly increases with redshift rather than with luminosity. A partial correlation analysis confirms that α_S is truly anticorrelated with redshift at the 99.9% confidence level, indicating evolution with cosmic epoch, and not a luminosity effect. Conversely, for α_H the observed anticorrelation with redshift is mostly due to a strong dependence on luminosity.

In radio-quiet quasars, we find marginal evidence for a flattening of α_H ($P = 4.5\%$), going from $z < 1$ to $z = 2$, in agreement with previous studies. Radio-loud quasars at $z < 2.2$ instead show a "concave" spectrum ($\alpha_H < \alpha_S$ by ~ 0.2). This new result is consistent with the widespread suggestion that the flatter X-ray spectra of radio-loud quasars may be due to an additional component above those seen in radio-quiet quasars. However, it might also imply different processes at work in radio-loud and radio-quiet sources. At $z \gtrsim 2$ the average soft and hard indices are similar and are both significantly smaller than at lower redshifts. This can be due to the soft component of radio-loud quasars being completely shifted out of the PSPC band at $z > 2$.

Subject headings: quasars: general — radio continuum: galaxies — X-rays: galaxies

1. INTRODUCTION

The ability of *ROSAT* to study fainter X-ray sources than ever before opened up the range of quasars that could be reached to span virtually the whole of their properties. High-redshift objects (up to $z \approx 4$) became accessible in X-rays, and their spectrum was measured for the first time between 0.4 and 10 keV (in the quasar frame; Elvis et al. 1994b). Unexpected low-energy cutoffs, far larger than those expected due to absorption by our Galaxy, were detected in several high-z radio-loud quasars (Wilkes et al. 1992; Elvis et al. 1994b). The obvious possibility was that these were caused by photoelectric absorption, either along the line of sight or at the quasar. If the absorber was at the quasar, then the material could be nuclear, as in low-redshift, low-luminosity objects (e.g., Elvis & Lawrence 1985; Elvis, Mathur, & Wilkes 1995) or could be on the larger scale of the host galaxy or protogalaxy. A tentative link with the highly compact "gigahertz peaked spectrum" radio sources suggested the latter and hence that X-ray astronomy offered a new probe of early galaxy conditions.

Targeted *ROSAT* studies of high-redshift quasar X-ray spectra are, however, limited to a dozen or so objects. Within the more than 3000 *ROSAT* PSPC pointings (covering about 10% of the sky) lie more than 50,000 sources (White, Giommi, & Angelini 1995; Voges et al. 1994). Out of these, a sample of several hundred quasar X-ray spectra can be readily compiled for the first time, thanks to the release of the two source catalogs WGACAT (White et al. 1995) and ROSATSRC (Voges et al. 1994). We have used these data to explore the questions raised by the initial PSPC high-redshift quasar studies. As an additional benefit of this program, we are able to study the emission spectra of a large sample of radio-loud and radio-quiet quasars and to study their differences.

We investigate the connection between low-energy X-ray cutoffs and the radio and optical spectra of these quasars in a companion paper (Elvis et al. 1998 [Paper II]). A later paper (Nicastro et al. 1997) will discuss a subsample of quasars selected to have the typical colors produced by absorption features imprinted on the X-ray spectrum by an ionized absorber along the line of sight.

We use a Friedmann cosmology with $H_0 = 50$ km s^{-1} Mpc^{-1} and $\Omega = 0$ throughout this paper.

2. THE SAMPLE

Quasars were selected by cross-correlating the first revision of the WGACAT (White et al. 1995) with a variety

[1] Harvard-Smithsonian Center for Astrophysics, 60 Garden Street, Cambridge MA 02138.
[2] Osservatorio Astronomico di Roma, Monteporzio (Rm), Italy.
[3] *BeppoSAX* Science Data Center, Rome, Italy.
[4] Dipartimento di Fisica, II Università di Roma "Tor Vergata," via della Ricerca Scientifica 1, I-00133 Rome, Italy.

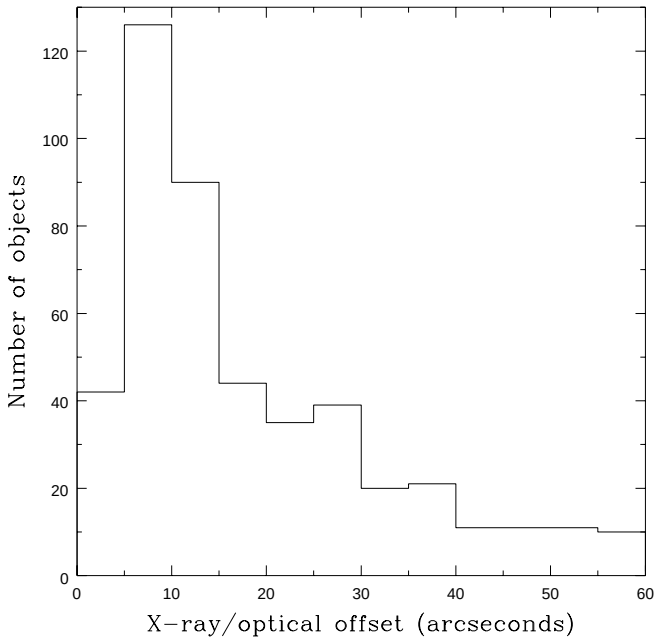

FIG. 1.—Distribution of X-ray/optical offsets for our sources, obtained by cross-correlating the WGACAT with various optical and radio catalogs with a correlation radius of 1′. The mean offset is $\simeq 18''$. The number of spurious associations is $\lesssim 2$ (see text for details).

of optical and radio catalogs, including the Véron-Cetty & Véron (1993) and Hewitt & Burbidge (1993) quasar catalogs, and the 1 Jy (Stickel, Meisenheimer, & Kühr 1994) and S4 (Stickel & Kühr 1994) radio catalogs. Uncertain classifications and borderline objects have also been checked in the NASA Extragalactic Database (NED).[5] All the objects selected have optical spectra dominated by nonstellar emission, and all show broad emission lines.

The maximum radius adopted for identifying cross-correlation candidates was 1′. The resulting distribution of X-ray/optical offsets is shown in Figure 1. The mean offset is $\simeq 18''$, while the median offset is $\simeq 13''$, in agreement with the estimated errors on the positions of the WGA sources (White et al. 1995). Potential misidentifications through chance coincidences were addressed by shifting the X-ray positions by various amounts several times, and repeating the cross-correlations. Using these randomized X-ray positions causes the chance coincidence rate to be small. The number of spurious X-ray/optical associations is at maximum 2, i.e., less than 0.5% of the whole sample (see below).

We excluded the following from the sample:

1. Observations of sources flagged in the WGACAT for quality less than 5 (corresponding to problematic detections).
2. Observations of sources with a signal-to-noise ratio in the 0.1–2.4 keV energy band less than 7 (to ensure reasonable X-ray color determinations).
3. Observations of quasars located at an off-axis angle larger than 45′ (to avoid large systematic errors due to the uncertainties in the PSPC calibration near the edge of the field of view).
4. Fields with a Galactic $N_{\rm H}$ along the line of sight higher than 6×10^{20} cm^{-2} (to ensure good low-energy signal-to-noise ratio).
5. Quasars with $z < 0.1$ (to eliminate the low-luminosity Seyfert galaxies in which absorption is common, e.g., Lawrence & Elvis 1982).

We are then left with 453 quasars for which fluxes in three bands, and so two X-ray colors ("soft" and "hard"), can be derived. This is the largest sample of quasars for which homogeneous X-ray spectral information is available. We used only one observation for each quasar. When more than one observation was available for a quasar, we chose the one with the highest signal-to-noise ratio.

Of these quasars, 202 have a radio measurement in the literature, and 167 of those are radio loud according to the usually adopted definition $R_L = \log (f_r/f_B) > 1$, with f_r the radio flux at 5 GHz and f_B the B-band flux (Wilkes & Elvis 1987; Kellermann et al. 1989; Stocke et al. 1992). This translates into a (rest-frame) value of the radio to optical spectral index, $\alpha_{ro} > 0.19$. The sample includes 87 flat-spectrum radio quasars ($\alpha_r < 0.5$), the majority of which are discussed by Padovani, Giommi, & Fiore (1997). Steep-spectrum radio quasars account for 62 sources. Note that this flat/steep classification is based mostly on the radio spectrum at only two or three frequencies. Quasars with complex radio spectra (e.g., gigahertz peaked spectrum [GPS] sources) could appear in either class. This classification also does not distinguish compact steep-spectrum (CSS) radio sources from extended ones. For 18 radio-loud quasars we could find radio measurements at one frequency only, and therefore their radio spectral index is unknown. We assumed $\alpha_R = 0.5$ in calculating α_{ro}. Most of the quasars without a radio measurement are likely to be radio-quiet (e.g., Ciliegi et al. 1995), so we include them in the radio-quiet sample, making for 286 radio-quiet quasars in the sample.

In the WGACAT there are another 35 quasars with Galactic $N_{\rm H} > 6 \times 10^{20}$ that in every other respect qualify

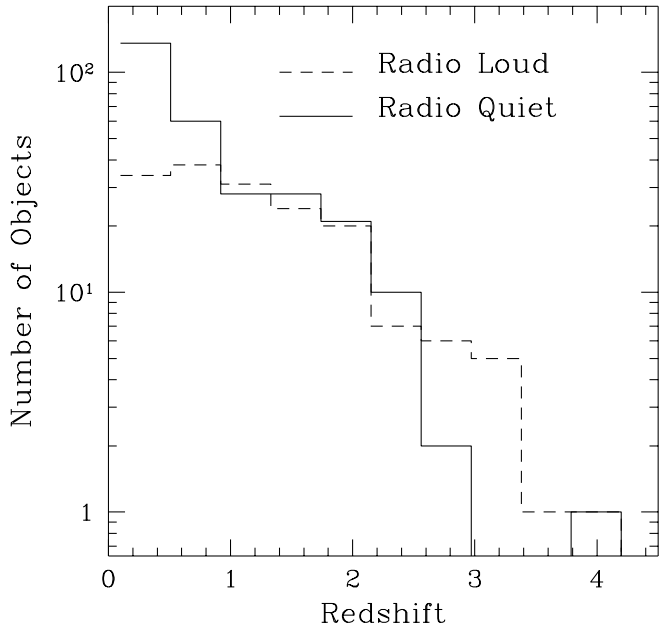

FIG. 2.—Redshift distribution of WGACAT radio-quiet quasars (*solid line*) and radio-loud quasars (*dashed line*) used in this paper.

[5] The NASA/IPAC Extragalactic Database (NED) is operated by the Jet Propulsion Laboratory, California Institute of Technology, under contract with the National Aeronautics and Space Administration.

as sample members for which we derive a "hard" color only. Of these, 28 are radio loud.

The redshift distributions for radio-quiet quasars and radio-loud quasars are shown in Figure 2. At $z \lesssim 1$ the number of radio-quiet objects is higher than that of radio-loud ones, owing to the higher volume density of radio-quiet quasars. By $z \gtrsim 2$, however, the number of radio-loud objects is higher than that of the radio-quiet objects, because of the higher L_X/L_{opt} of radio-loud quasars.

3. EFFECTIVE X-RAY SPECTRAL INDICES

The WGACAT provides raw count rates in three energy bands: 0.1–0.4 keV (soft band), 0.40–0.86 keV (medium band) and 0.87–2 keV (hard band) for each entry. The count rates can be combined to form a "softness ratio" (SR = soft/medium) and a "hardness ratio" (HR = hard/medium). To allow for the effect of the varying Galactic absorption from source to source, these softness and hardness ratios can be converted to "effective spectral energy indices," α_S (0.1–0.8 keV), and α_H (0.4–2.4 keV), assuming the Galactic N_H as derived from 21 cm measurements (Stark et al. 1992; Heiles & Cleary 1979), "Wisconsin" cross sections (Morrison & McCammon 1983) and solar abundances (Anders & Ebihara 1982), and measurements using the PSPC calibration[6].

3.1. *Correction for the Instrumental Point-Spread Function*

In converting the three count rates into effective spectral indices, corrections must be applied for the instrumental point-spread function (PSF), to take into account the different fraction of counts lost outside the detection region in each energy band. The total PSPC PSF includes two main components: the mirror PSF and the PSPC detector PSF (Hasinger et al. 1992). The mirror PSF is energy independent, and dominates the total PSF at off-axis angles greater than about 20′. At these large off-axis angles a small detection region loses flux but does not significantly alter the spectral shape.

The detector PSF is, instead, highly energy dependent, and dominates the total PSF at small off-axis angles. Using a small detection region for an off-axis angle less than 20′ can strongly alter the spectral shape, predominantly at low energies. (The detector FWHM is proportional to $E^{-0.5}$). The method used in the WGACAT to estimate the source count rates uses the counts detected in a box whose size optimizes the signal-to-noise ratio for each source. For relatively weak sources near the field center, this optimum box size is small, and the number of soft photons lost is greater than that of medium or hard photons, giving rise to an artificial reduction of the spectrum at low energies, which in turn can lead to an underestimation of α_S of up to 0.2–0.3.

We corrected the count rates in the three bands for both mirror and PSPC PSF effects. We used the analytical approximations for the energy and off-axis angle dependence of the PSF provided by Hasinger et al. (1992).

This method of estimating spectral indices is similar to the dereddening procedure used in optical photometry, and is quite robust, with typical systematic uncertainties on α_H smaller than 0.1 (as shown, for example, by Padovani & Giommi 1996 or Ciliegi & Maccacaro 1996). It is particularly suitable for handling large samples of objects (Giommi et al. 1998, in preparation), e.g., for the determination of the X-ray spectral index distributions.

However, a systematic uncertainty remains in the spectral index estimates, because the magnitude of the PSF correction depends on the intrinsic source spectrum. To estimate the magnitude of this uncertainty, we calculated five series of values of α_S and α_H for a grid of assumed source spectra: for the average value for a high Galactic latitude line of sight ($N_H = 3 \times 10^{20}$ cm^{-2}) we used $\alpha_E = 1$, $\alpha_E = 1.5$, and $\alpha_E = 2.5$; for the mean value of the energy spectral index ($\alpha_E = 1.5$) we used low ($N_H = 10^{20}$ cm^{-2}) and high ($N_H = 10^{21}$ cm^{-2}) absorption values. We then calculated the differences between the α_S and α_H calculated for each pair of α_E and N_H and those calculated for $\alpha_E = 1.5$ and $N_H = 3 \times 10^{20}$ cm^{-2}. The differences in α_H were always smaller than 0.05, and those in α_S were always smaller than 0.15. We therefore use these values as systematic uncertainties in the evaluation of these parameters.

3.2. *Correction for PSPC Background*

The WGACAT count rates are not background subtracted. Therefore, another possible source of error in the evaluation of the PSPC spectral indices is the PSPC background in the three WGACAT bands. The PSPC background has been studied in great detail by Snowden et al. (1992, 1994 [non–cosmic background] and 1995, 1997 [diffuse, cosmic X-ray background]) using *ROSAT* All Sky Survey (RASS) data and pointed observation data. The energy band that shows, by far, the highest background at high Galactic latitude is the 0.1–0.28 keV range, which spans most of the soft band defined in WGACAT (0.1–0.4 keV) We now analyze the effect that a wrong or absent background subtraction in the soft band can have on the soft energy index α_S.

The cosmic background in the soft band is spatially variable by a factor of 5, with large regions of maxima of about 0.0015 counts s^{-1} arcmin^{-2} at high Galactic latitudes ($b > 30°$) and minima of 0.0003 counts s^{-1} arcmin^{-2}. Long-term enhancements are difficult to identify and model in pointed observations. They mainly affect the low-energy part of the spectrum, $E < 0.28$ keV, where their contribution can even be as high as 0.001 counts s^{-1} arcmin^{-2}. We adopt a conservative value for the total soft band background of 0.003 counts s^{-1} arcmin^{-2}.

The typical box side of the WGACAT extraction regions is 0.′3–0.′8 for off-axis angles smaller than 20′ and 1′–3′ for off-axis angles between 20′ and 45′, where the lower limits apply to the faintest sources. Such extraction regions, together with the above background rate, would give a few counts in the low-energy band in typical exposures of 1000–10,000 s for sources detected in the central 20′, and a few tens of counts for sources detected in the outer PSPC region.

Let us assume the case of a faint (close to our limit of 7 in signal-to-noise ratio) and strongly cut-off source, whose counts in the soft band are a few, comparable to the background contribution, and 15–30 in the medium band. In this case the upper limit on the slope between the soft and medium energy bands differs from the slope we would measure neglecting background subtraction by ~ 0.5. This compares with a typical statistical error in α_S of 0.5–0.7 for such faint sources and with a systematic uncertainty of 0.15. We conclude that the small extraction regions used in the WGACAT means that background is not a significant

[6] A table of the count rates and effective X-ray spectral indices can be obtained via anonymous ftp at www.sdc.asi.it, cd /pub/ff/wga.

problem, even for the soft band count rate of our faint sources. As a result we did not subtract background in the evaluation of the effective spectral indices α_S and α_H.

To investigate the robustness of this assumption, we searched for correlations between the soft and hard effective spectral indices and (1) the size of the extraction region, (2) the off-axis angle, and (3) the source count rate. Any correlations would be evidence that neglecting the background was causing problems. In no case did we find significant correlations. We conclude that neglecting the background subtraction does not strongly affect or bias our results.

There are two other sources of uncertainties in the spectral index estimates: first, quasars located near the PSPC rib structures can suffer a preferential loss of soft photons. We inspected the original *ROSAT* images for each source that appeared to have unusually low soft band counts and rejected those that might have been so affected. Second, the spectral index estimates from hardness ratios may be significantly different from the results of a proper spectral fit to the full pulse-height analyzer (PHA) spectrum, in the presence of a curvature in the intrinsic spectrum, because of the skewness induced in the broad energy bands used to construct the hardness ratios. For all these reasons the effective spectral indices α_S and α_H should not be regarded as a measure of the true emission spectral indices. They should rather be regarded as a rough estimation of the "average" soft and hard spectral shapes. They are the soft X-ray analogs of $(U-B)$, $(B-V)$ colors, for which multiple physical interpretations are possible. We will use α_S as an indicator of a possible low-energy cutoff.

4. EFFECTIVE SPECTRAL INDICES AND QUASAR PROPERTIES

Armed with these effective X-ray spectral indices, we can now examine their dependence on quasar type, redshift, and luminosity.

The radio-quiet and radio-loud quasars α_S and α_H are plotted against each other in Figures 3*a* and 3*b*. In the radio-loud plot, flat-spectrum radio sources are identified by circles, and steep-spectrum sources by squares. High-redshift quasars ($z > 2.2$) are shown with filled symbols. The ranges of α_S and α_H are large, and so the different parts of the diagram correspond to radically different spectral shapes. These are illustrated with three-point spectra in Figure 3. For the purpose of this paper we are most interested in those for which a low-energy cutoff is indicated (Fig. 3, *lower center*).

To study these features more closely, we divided the quasars into four redshift bins: 0.1–0.5; 0.5–1; 1–2.2; and above 2.2. Table 1 gives the average spectral indices (α_S, α_H) and their dispersions [$\sigma(\alpha_S)$, $\sigma(\alpha_H)$] in these four redshift bins for both radio-quiet and radio-loud quasars. The typical statistical uncertainties on α_S and α_H are ± 0.2, and the systematic uncertainty is at most ± 0.15 for α_S and ± 0.05 for α_H, so the measured dispersions are not strongly affected by these uncertainties.

4.1. *Radio-loud versus Radio-quiet*

The mean and dispersion of α_H and α_S for the radio-quiet quasars are (1.59, 0.52) and (1.69, 0.41); those of radio-loud quasars are (1.13, 0.55) and (1.32, 0.59). The difference of ~ 0.5 in α_H agrees with the widespread finding that radio-loud quasars have flatter X-ray spectra than radio-quiet quasars (e.g., Wilkes & Elvis 1987; Laor et al. 1997, 1994; Schartel et al. 1996a).

For radio-quiet quasars the distribution of α_S is consistent with that of α_H in all redshift bins. In the last redshift bin there are only 12 quasars (see Table 1), and only three at $z > 2.5$, and therefore the test is not very stringent for this redshift interval. This uniformity suggests a single emission mechanism dominating the whole *ROSAT* band (cf. Laor et al. 1997), at least for redshifts smaller than about 2.

Radio-loud quasars, instead, have α_H smaller than α_S by ~ 0.2 (i.e., a concave spectrum) in the low-redshift bins

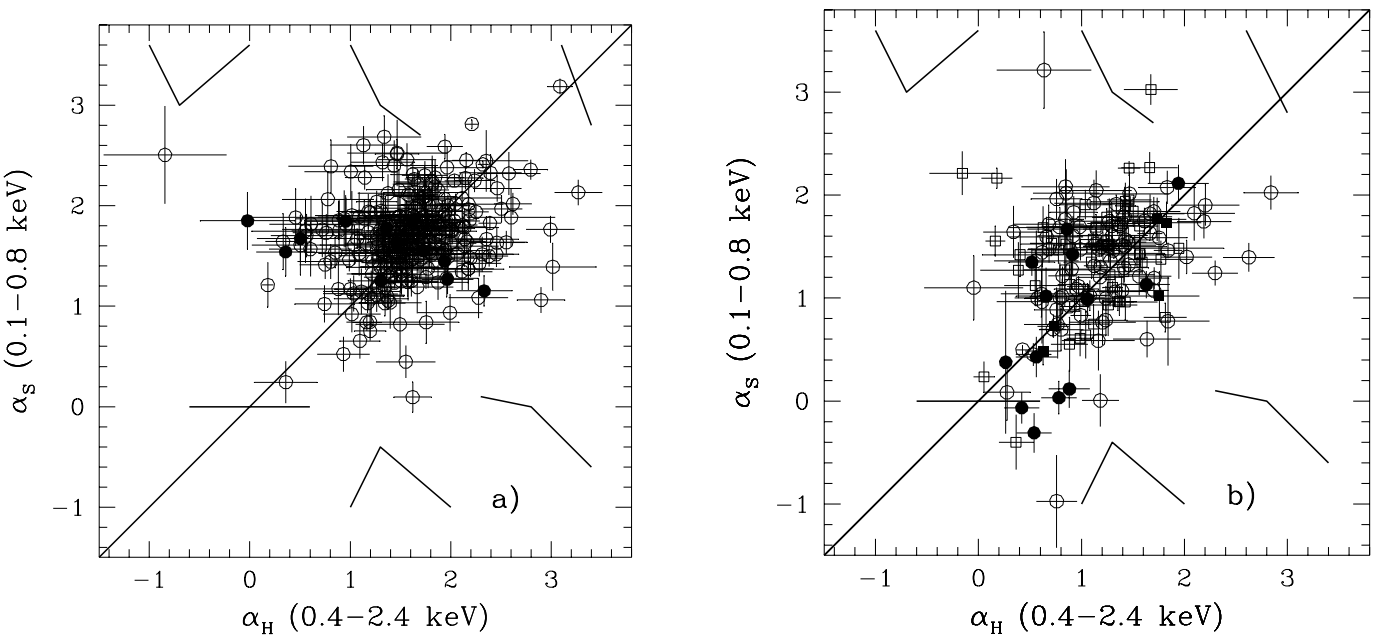

FIG. 3.—"Soft" effective spectral index (α_S) plotted against the "hard" effective spectral index (α_H) for (*a*) radio-quiet quasars, and (*b*) radio-loud quasars. Radio-loud flat-spectrum radio sources are identified by circles, steep radio spectrum sources by squares. High-redshift quasars ($z > 2.2$) are shown with filled symbols. Three-point spectra illustrate the radically different spectral shapes in different parts of the diagrams.

TABLE 1

QUASAR AVERAGE SPECTRAL INDICES AND CUTOFF STATISTICS

Redshift Bin	N	α_S	$\sigma(\alpha_S)$	N	α_H	$\sigma(\alpha_H)$	Number of Cutoffs	Fraction
Radio-quiet Quasars								
0.1–0.5	136	1.73	0.48	141	1.62	0.51	7	0.051
0.5–1.0	66	1.68	0.36	67	1.67	0.51	3	0.045
1.0–2.2	72	1.67	0.38	72	1.51	0.49	1	0.014
>2.2	12	1.54	0.26	13	1.32	0.69	0	0
Radio-loud Quasars								
0.1–0.5	34	1.49	0.52	41	1.20	0.63	1	0.029
0.5–1.0	45	1.30	0.62	51	1.18	0.48	2	0.044
1.0–2.2	70	1.37	0.52	78	1.13	0.51	4	0.057
>2.2	18	0.89	0.71	25	0.89	0.60	7	0.389
Flat-Spectrum Radio Quasars								
0.1–0.5	9	1.38	0.30	14	1.32	0.38	...	...
0.5–1.0	26	1.24	0.73	30	1.11	0.51	...	...
1.0–2.2	40	1.35	0.50	43	0.99	0.46	...	...
>2.2	12	0.74	0.75	17	0.78	0.60	...	...
>0.1	87	1.24	0.63	104	1.04	0.51	...	...
Steep-Spectrum Radio Quasars								
0.1–0.5	19	1.52	0.62	21	0.96	0.65	...	...
0.5–1.0	14	1.29	0.44	16	1.23	0.39	...	...
1.0–2.2	24	1.40	0.58	28	1.12	0.46	...	...
>2.2	5	1.15	0.58	7	1.33	0.60	...	...
>0.1	62	1.37	0.56	72	1.14	0.56	...	...

($z < 2.2$). The Kolmogorov-Smirnov (KS) probability of α_S being drawn from the same distribution function as α_H is 5.0% for redshifts 0.1–0.5, 22% for redshifts 0.5–1.0, and 0.14 % for redshifts 1.0–2.2. This new result could be interpreted in terms of an additional component in the spectrum of radio-loud quasars above that seen in radio-quiet quasars (as suggested earlier by, e.g., Wilkes & Elvis 1987). However, it may also imply different processes at work in radio-loud and radio-quiet quasars (as also suggested by Laor et al. 1997). To disentangle these two possibilities, a careful analysis of the optical to X-ray spectral energy distribution of WGACAT quasars is needed. This is beyond the scope of this paper and will be addressed in a forthcoming paper.

We have computed the mean α_S and α_H for the two samples of flat and steep radio spectrum quasars. These are reported in Table 1. Although both distributions of α_S and α_H for the steep- and flat-spectrum radio quasars are consistent with being drawn from the same distribution function (using a KS test), the mean α_S of steep radio spectrum quasars is steeper than that of flat radio spectrum quasars (at the 90% confidence level). The mean α_H of the two samples of quasars is, on the other hand, very similar. Redshift bins 0.1–0.5 and $z > 2.2$ are populated by too small a number of flat radio spectrum and steep radio spectrum quasars, respectively, to allow a statistically significant comparison. In the other two redshift bins the distributions of α_H and α_S of the two samples are consistent with each other.

The dispersion in α_H and α_S is large for both radio-quiet and radio-loud quasars.

The radio-loud dispersion in α_S is larger than that of radio-quiet quasars at a confidence level of 96%. Emission or absorption mechanisms that produce more varied outputs seem to be needed for radio-loud quasars.

From Figure 3 it appears that the number of radio-loud quasars with $\alpha_S < 0.5$ is much larger than the number of radio-quiet quasars with $\alpha_S < 0.5$, especially at high z (*filled symbols*). This is the sense of the change in α_S to produce low-energy cutoffs, as would be produced by photoelectric absorption.

We compare the distribution of radio-loud and radio-quiet indices about their respective mean values of α_S (Fig. 4). By offsetting from the mean of each group, we remove the difference in the group means discussed above. Figure 4 shows the broader dispersion of α_S for radio-loud quasars. It also shows a population of radio-loud quasars with smaller α_S, i.e., quasars that show low-energy cutoffs. This tells us with high confidence that the cutoffs are not due to intervening material. Intervening material would not "know" whether a background quasar was radio loud or radio quiet. The cause of the cutoffs must be physically associated with the quasar in some way.

4.2. *Dependence on Redshift*

To search for changes with redshift and study their evolution, we plot α_H and α_S versus redshift for radio-quiet and radio-loud quasars in Figures 5*a* and 5*b* and Figures 6*a* and 6*b*, respectively. There is no strong evidence of evolution of either α_H or α_S with redshift for radio-quiet quasars. Again, the small number of radio-quiet quasars with $z > 2$ does not allow us to draw a strong conclusion for high-redshift objects. For the bins $0.5 < z < 1$ and $1 < z < 2.2$ the probability that the two distributions of α_H are drawn from the same distribution function is marginally unacceptable ($P = 4.5\%$), in agreement with previous studies (Schartel et al. 1996b).

On the other hand, radio-loud quasars show strong changes in both α_S and α_H for $z > 2.2$, in the sense that both

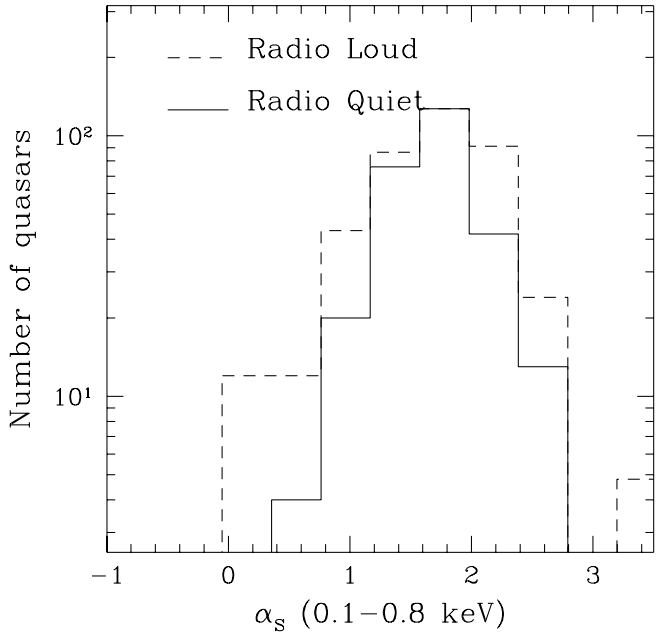

FIG. 4.—Distribution of radio-loud (*dashed line*) and radio-quiet (*solid line*) indices about their respective mean α_S. The mean of radio-loud quasars has been offset to coincide at $\alpha_S = 1.7$ with that of radio-quiet quasars. The radio-loud distribution has been normalized to the maximum of the radio-quiet distribution.

indices are smaller than in lower redshift bins. We ran a KS test between the distributions of spectral indices in each possible pair formed with the four redshift bins. The distributions of α_S and α_H at $z < 2.2$ are all consistent with one another. Only the $z > 2.2$ bin shows significant differences from the others, for both α_S and α_H. Table 2 gives the percentage probability that the spectral index distributions of α_S and α_H in two redshift bins are drawn from the same distribution function.

TABLE 2

KOLMOGOROV-SMIRNOV TEST FOR RADIO-LOUD QUASARS

Redshift Bin	0.1–0.5	0.5–1.0	1.0–2.2	>2.2
		α_S		
>2.2	3.0	5.8	2.1	...
		α_H		
>2.2	0.10	4.1	0.16	...

Some caution is required, however. In flux-limited samples redshift and luminosity are often degenerate, so that it is hard to distinguish the effects of one from those of the other. The apparent trend with redshift discussed above may thus be induced by a correlation with luminosity (Fig. 7*a*). We tested for this degeneracy by selecting a subsample of only the high log $L_{\rm opt}$ (>32) quasars. The correlation between α_S and z for this sample is still very good (Fig. 7*b*; linear correlation coefficient $r = -0.46$, which, for 43 points, corresponds to a probability of 99.8%). On the other hand, the correlation between α_H and z for the high-luminosity, high-redshift quasar is not significant, $r = -0.17$ (probability of 72%).

To better disentangle the luminosity/redshift dependence of α_S and α_H, we also performed a partial correlation analysis (e.g., Kendall & Stuart 1979) on the whole radio-loud sample. While α_S is anticorrelated with redshift even after subtraction of the effect of the optical luminosity ($P \simeq 99.9\%$), in the case of α_H no correlation with redshift is left once the luminosity dependence is subtracted out ($\simeq 48\%$). On the other hand, excluding the redshift dependence, we find that α_H is anticorrelated with luminosity at the 99.2% level.

We conclude that the "cutoff" α_S spectra, unlike the α_H spectra, are truly more common at high redshifts, and so are an evolutionary, or cosmological, effect.

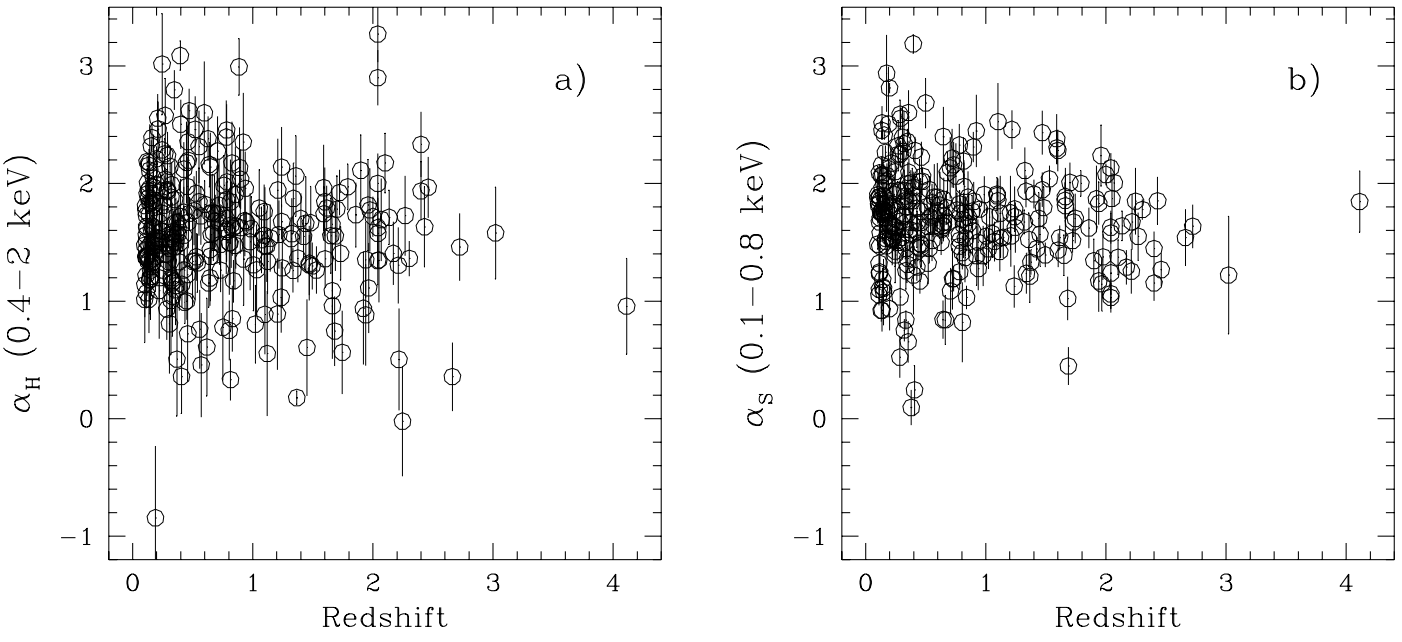

FIG. 5.—(*a*) α_H and (*b*) α_S plotted against the redshift for radio-quiet quasars

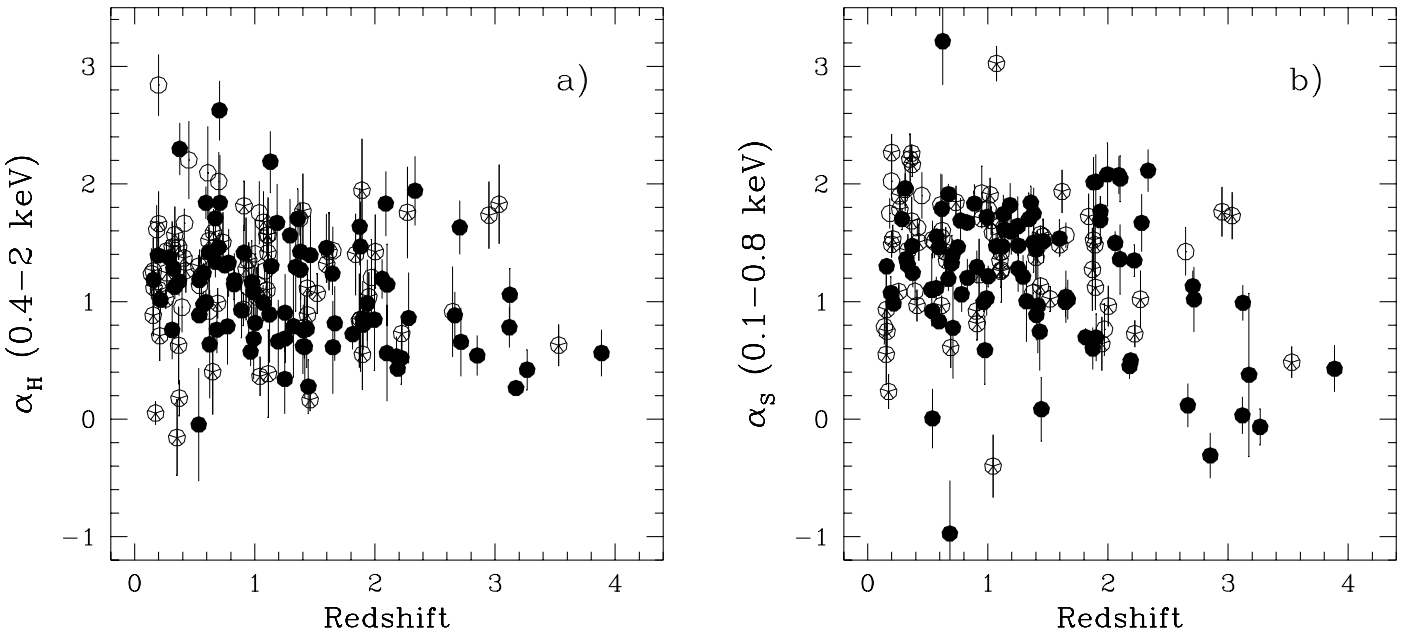

FIG. 6.—(*a*) α_H and (*b*) α_S plotted against the redshift for radio-loud quasars. Filled circles identify flat radio spectrum quasars. Starred circles identify steep radio spectrum quasars.

4.3. *Low- Energy Cutoffs*

The high incidence of low-energy cutoffs at high redshifts can be made clearer by defining a sample of "candidate cutoff" objects using α_S and then examining the fraction that occur among both radio-loud and radio-quiet quasars as a function of redshift.

The change in index of radio-loud quasars can be seen in Figure 6*b* as due to a population of radio-loud quasars with a soft spectral index significantly smaller than the average and smaller than the hard spectral index (although there are also a few radio-quiet quasars with exceptionally flat α_S; Fig. 5*b*). These small α_S quasars are "cut off" in their low-energy spectrum compared with an extrapolation of the hard spectrum.

We select "candidate" low-energy cutoff quasars using three criteria: (1) $\alpha_S < \alpha_H$. (2) $\alpha_S < 0.5$ selects all the high-redshift radio-loud candidates apparent in Figure 6*b*. (3) Lower redshift radio-loud and all radio-quiet candidates require a more careful selection, since their mean values of α_S are different. We use the criterion that they have α_S smaller than the average by at least 0.75. For radio-loud quasars the average α_S at $z < 2.2$ is 1.32, and therefore we selected quasars with $\alpha_S < 0.58$ in this redshift interval. For radio-quiet quasars there is no evidence for a change in the average α_S with z, and therefore we selected the quasars with $\alpha_S < 0.94$ (the average α_S is 1.69). These criteria select 10 radio-quiet and 14 radio-loud candidate cutoff quasars. Table 3 gives the optical or radio names, redshifts, and optical luminosities of these objects.

The distribution of candidate cutoffs is striking. Table 1 gives the total number of quasars, the number of candidate cutoff quasars, and its fraction in each redshift bin, while

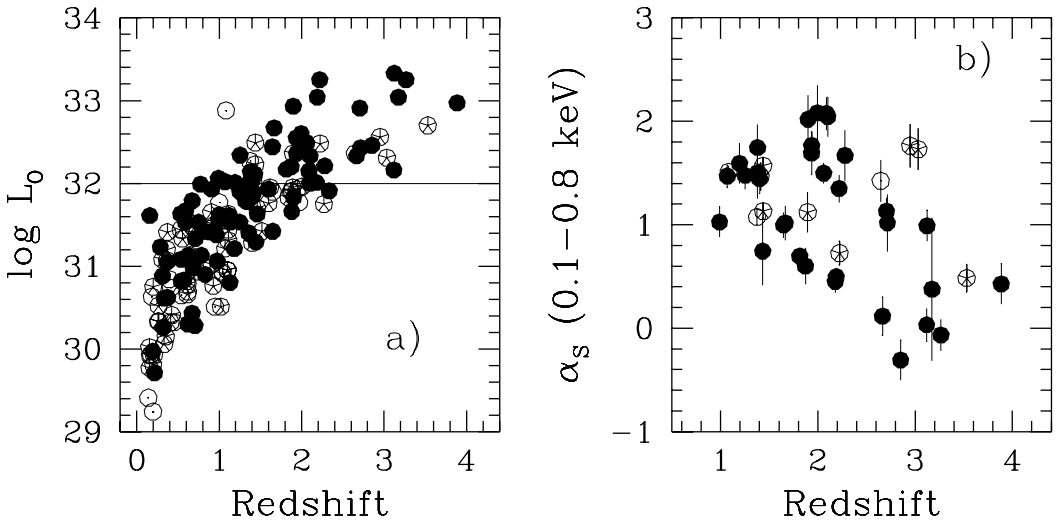

FIG. 7.—(*a*) Redshift–optical luminosity correlation for radio-loud quasars. (*b*) Soft spectral index α_S–redshift correlation for radio-loud quasars with high optical luminosity ($> 10^{32}$ ergs s^{-1}).

TABLE 3

"CANDIDATE" CUTOFF QUASARS

Quasar	z	log L_{opt} (ergs s^{-1})
Radio Quiet		
RXJ 16331+4157.....	0.136	29.14
MS 02388−2314	0.284	29.92
Q0335−350	0.321	29.68
MS 03363−2546	0.334	30.20
US 3333	0.354	30.55
PHL 6625[a]	0.38	29.98
MS 12186+7522	0.645	30.77
Q1234+1217.....	0.664	30.67
MS 21340+0018	0.805	30.31
SBS 0954+495.....	1.687	31.32
Radio Loud		
3C 219	0.174	29.93
PKS 1334−127.....	0.539	31.08
3C 207	0.684	30.98
3C 212	1.043	30.91
S4 0917+624	1.446	31.29
S4 0917+449	2.18	32.01
4C 71.07[b]	2.19	33.04
PKS 2351−154.....	2.665	32.33
PKS 0438−43	2.852	32.46
PKS 0537−286.....	3.119	32.16
S4 0636+680	3.174	33.04
PKS 2126−158.....	3.266	33.25
PKS 1442+101.....	3.53	32.7
S4 1745+624	3.886	32.97

[a] 4.′6 from NGC 247 nucleus.
[b] Blazar; EGRET.

Figure 8 shows the fraction of candidate cutoff quasars as a function of z for both quasar samples. The fraction of candidate cutoff quasars among the 18 radio-loud objects at $z > 2.2$ is significantly different from that at $z < 2.2$ (probability of 0.002%, using the binomial distribution). For radio-quiet objects the absence of cutoffs among the 12 quasars at $z > 2.2$ is consistent with the cutoff distribution at lower redshift (probability of 50%). In turn, the probability of finding zero candidate cutoff quasars among the $n = 12$ radio-quiet quasars at $z > 2.2$, assuming a frequency of cutoffs similar to that of radio-loud quasars at the same redshift, is 0.3%.

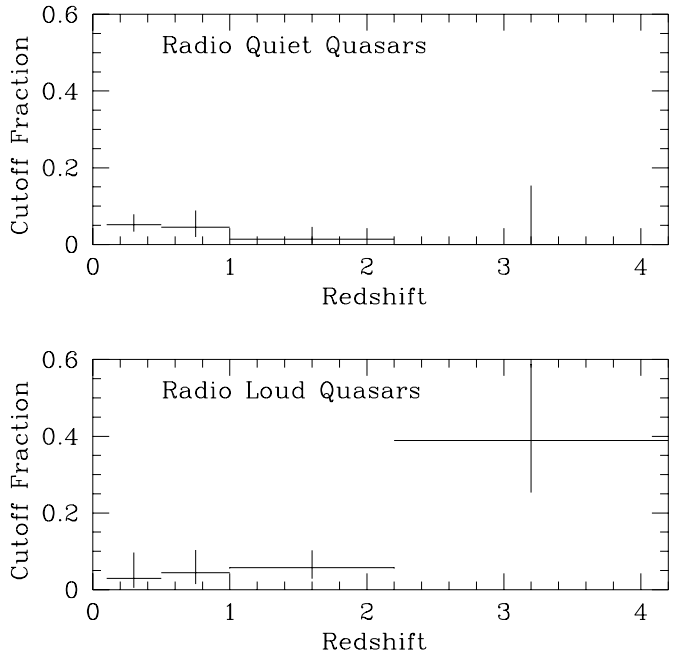

FIG. 8.—Fraction of "candidate" cutoff quasars as a function of the redshift for radio-quiet quasars (*upper panel*) and radio-loud quasars (*bottom panel*).

This strongly suggests a difference in the candidate cutoff quasar distribution with z between radio-loud and radio-quiet objects. We calculated, using the Fisher exact probability test (e.g., Siegel 1956), the probability that the two candidate cutoff samples differ in the proportion in which they are distributed in redshift, e.g., below and above a given redshift. For $z = 2.2$ the difference is significant at the 98.4% level.

5. X-RAY SPECTRA

A flatter α_S at high redshift than at low redshift can be due to at least three effects: (*a*) the redshifting of a soft component contributing to the emission below $\approx$1–3 keV (quasar frame) out of the observed energy range for $z \gtrsim 2$; (*b*) evolution of the emission spectrum; (*c*) a cutoff due to low-energy absorption becoming more frequent at $z \gtrsim 2$. A simple color analysis cannot distinguish between these three possibilities. A two-parameter spectral fit can discriminate more strongly, and is possible for the quasars with a few hundred detected PSPC counts. This section investigates such fits.

Most of the quasars in the sample do not have published PSPC spectral fits.

We extracted the full pulse-height spectrum for each of the quasars in the sample from the appropriate event files in the *ROSAT* archive. We used standard extraction criteria (see, e.g., Fiore et al. 1994; Elvis et al. 1994b). Table 4 gives the total counts in the 0.1–2.4 keV energy band, the exposure, and the off-axis angle for these quasars. All the radio-loud quasars were observed on-axis and were the targets of observation. All the radio-quiet quasars (except RXJ 16331+4157) are instead serendipitous sources in *ROSAT* fields. With one exception (SBS 0945+495), the radio-quiet quasars all lay within the inner PSPC rib ($r = 18'$), where the calibration is most accurate.

We then fitted the spectra with a power-law model with low-energy absorption (at $z = 0$). We made four fits for each quasar: We first let the column density be free to vary, and then kept it fixed to the Galactic (21 cm) value along the line of sight. Similarly, we let the power-law spectral index be free to vary, and then kept it fixed to the mean value of α_H at the redshift of the quasar (Table 1). The results are given in Tables 5 and 6 for each quasar sample. Listed are the best-fit parameters, the value of χ^2, and the probability that the improvement in χ^2 between the fits with free N_H and N_H fixed to the Galactic value is significant (calculated using the χ^2 distribution with 1 dof for $\Delta\chi^2$).

From Tables 5 and 6 we see that the evidence of a cutoff is very robust ("class A") for four radio-loud quasars (PKS 2126−158, PKS 0438−436, 3C 212, and 3C 207 [$P \gtrsim 99.9\%$]).

For another four radio-loud quasars (S4 1745+624, PKS 2351−154, S4 0917+449, and PKS 1334−127) the probability of a cutoff is $\gtrsim$95% ("class B").

For S4 0917+624 the probability of a cutoff is $\gtrsim$92% ("class C").

TABLE 4

"CANDIDATE" CUTOFF QUASARS: PSPC OBSERVATIONS

Quasar	Counts	Exposure (s)	Off-Axis Angle (arcmin)
	Radio Quiet		
RXJ 16331+4157.....	281	13636	On
MS 02388−2314	223	8008	16.4
Q0335−350	744	17957	13.0
MS 03363−2546	938	50058	18.7
US 3333	416	11863	13.2
PHL 6625	328	19072	3.0
MS 12186+7522	321	6484	14.6
Q1234+1217.....	114	9426	13.5
MS 21340+0018	86	5201	11.6
SBS 0954+495.....	182	3669	35
	Radio Loud		
3C 219	509	4386	On
PKS 1334−127.....	516	3614	On
3C 207	452	7017	On
3C 212	770	21565	On
S4 0917+624	366	19465	On
S4 0917+449	640	3367	On
4C 71.07	5254	6993	On
PKS 2351−154.....	419	6335	On
PKS 0438−43	163	21231	On
PKS 0537−286.....	555	9487	On
S4 0636+680	68	5342	On
PKS 2126−158.....	1262	7392	On
PKS 1442+101.....	655	15433	On
S4 1745+624	506	16141	On

Furthermore, three quasars (3C 219, PKS 0537−286, and S4 0636+680) have very flat energy indices, much flatter than the average for radio-loud quasars at those redshifts, if we insist on only Galactic absorption (we also call these "class C"). Excess absorption, similar to that required in the better spectra, readily produces a normal energy index.

Two radio-loud quasars do not show any evidence for a cutoff (4C 71.07 and PKS 1442+101). The first is a famous blazar, detected by EGRET in the GeV energies (e.g., von Montigny et al. 1995), and therefore beaming is important. The second is often classified as a compact steep radio spectrum quasar (e.g., Dalla Casa et al. 1995).

The total number of cutoff radio-loud quasars is therefore eight, with three more objects likely to be cutoff quasars.

By contrast, in radio-quiet quasars we have strong evidence for a cutoff in only one case out of 289 (PHL 6625; $P > 99.9\%$). PHL 6625 lies just 4.'6 from the position of the low-redshift galaxy NGC 247. The cutoff in PHL 6625 may well be due to absorption in gas associated with NGC 247 (Elvis et al. 1998b). Two other radio-quiet quasars MS 03363−2546, US 3333) have a probability for a cutoff $\gtrsim 95\%$. US 3333 is included in the area of the sky already surveyed by the NVSS (Condon et al. 1998) but has not been detected. The upper limit on the radio flux ($f_r < 2.5$ mJy) puts an upper limit of 0.2 on α_{ro}, very close to the threshold of 0.19 that we use to divide radio-loud and radio-quiet quasars. More sensitive optical and radio

TABLE 5

CANDIDATE CUTOFF RADIO-QUIET QUASARS: SPECTRAL FITS

Quasar	$N_{H,Gal}$ (10^{20} cm^{-2})	N_H (10^{20} cm^{-2})	α_E	χ^2/dof	$P(\Delta\chi^2)$ (%)
RXJ 16331+4157.....	1.05	$1.1^{+2.1}_{-1.1}$	$0.87^{+0.80}_{-0.60}$	7.0/13	
		$2.7^{+0.8}_{-0.4}$	1.6 fixed	9.2/14	...
MS 02388−2314	2.29	$5.5^{+7.3}_{-3.1}$	1.0 ± 0.8	4.8/14	
		2.29 fixed	0.32 ± 0.25	5.9/15	...
		$8.2^{+3.8}_{-3.0}$	1.6 fixed	5.9/15	...
Q0335−350	1.26	$2.1^{+1.0}_{-0.8}$	1.18 ± 0.35	14.8/23	
		1.26 fixed	0.86 ± 0.08	17.2/24	...
		3.1 ± 0.3	1.6 fixed	17.6/24	...
MS 03363−2546	1.05	$2.1^{+1.8}_{-0.8}$	1.28 ± 0.30	72.6/67	
		1.05 fixed	0.89 ± 0.06	77.4/68	97.2
		2.9 ± 0.2	1.6 fixed	74.3/68	
US 3333	4.36	$7.7^{+5.1}_{-2.5}$	1.36 ± 0.55	8.2/15	
		4.36 fixed	0.77 ± 0.14	12.8/16	96.8
		9.0 ± 0.2	1.6 fixed	8.7/16	...
PHL 6625	1.47	$7.7^{+3.0}_{-2.8}$	1.88 ± 0.6	2.5/12	
		1.47 fixed	0.32 ± 0.14	19.3/12	99.995
MS 12186+7522	3.02	3.0 fixed	0.7 ± 0.5	5.7/11	
		$6.5^{+1.7}_{-1.0}$	1.6 fixed	9.5/12	...
Q1234+1217.....	2.51	$4.5^{+9.1}_{-3.1}$	$1.5^{+1.6}_{-0.5}$	3.4/6	
		2.51 fixed	0.93 ± 0.33	3.8/7	...
MS 21340+0018	4.00	$2.7^{+18.3}_{-2.7}$	$0.6^{+1.5}_{-0.3}$	0.71/5	
		4.0 fixed	0.90 ± 0.45	0.81/6	...
		$6.2^{+6.4}_{-1.7}$	1.6 fixed	1.62/6	...
SBS 0954+495.....	0.87	$5.2^{+6.8}_{-5.2}$	2.0 ± 2.0	6.5/7	
		0.87 fixed	0.57 ± 0.30	7.9/8	...
		$4.0^{+1.4}_{-1.0}$	1.6 fixed	6.6/8	...

TABLE 6

CANDIDATE CUTOFF RADIO-LOUD QUASARS: SPECTRAL FITS

Quasar	$N_{H,Gal}$ (10^{20} cm^{-2})	N_H (10^{20} cm^{-2})	α_E	χ^2/dof	$P(\Delta\chi^2)$ (%)
3C 219	1.48	$2.1^{+0.8}_{-1.2}$	0.22 ± 0.40	6.3/22	
		1.48 fixed	0.05 ± 0.10	6.8/23	...
		$5.7^{+0.7}_{-0.5}$	1.34 fixed	23.0/23	
PKS 1334−127.....	4.41	$7.1^{+3.0}_{-2.0}$	1.2 ± 0.4	11.0/20	
		4.41 fixed	0.66 ± 0.13	15.3/21	96.2
3C 207	4.07	$29^{+30}_{-21.5}$	2.3 ± 1.4	13.6/17	
		4.07 fixed	0.34 ± 0.16	24.9/18	99.92
3C 212	3.70	32^{+18}_{-16}	1.9 ± 1.0	14.4/21	
		3.70 fixed	0.14 ± 0.09	32.0/22	99.997
S4 0917+624	3.55	$11.9^{+32}_{-7.9}$	0.46 ± 0.30	5.0/14	
		3.55 fixed	0.76 ± 0.21	8.25/15	92.6
S4 0917+449	1.51	$2.9^{+1.2}_{-1.0}$	0.79 ± 0.33	17.6/22	
		1.51 fixed	0.37 ± 0.08	22.1/23	96.6
4C 71.07	2.95	3.3 ± 0.3	0.52 ± 0.09	26.4/29	
		2.95 fixed	0.43 ± 0.03	28.9/30	...
PKS 2351−154.....	2.39	$5.4^{+3.5}_{-1.2}$	0.87 ± 0.49	12.6/19	
		2.39 fixed	0.25 ± 0.14	17.3/20	97.0
PKS 0438−43	1.50	$6.9^{+3.5}_{-1.8}$	$0.70^{+0.27}_{-0.22}$	10.3/22	
		1.5 fixed	-0.16 ± 0.06	55.4/23	>99.999
PKS 0537−286.....	2.06	$2.7^{+1.7}_{-1.4}$	0.38 ± 38	16.2/22	
		2.06 fixed	0.22 ± 0.11	16.8/23	...
		3.8 ± 0.5	0.7 fixed	17.8/23	...
S4 0636+680	5.7	5.7 fixed	-0.1 ± 0.4	10.64/15	
		20^{+10}_{-8}	1.7 fixed	9.52/15	
PKS 2126−158.....	4.85	$12.9^{+7.2}_{-3.8}$	$0.70^{+0.41}_{-0.29}$	20.6/20	
		4.85 fixed	-0.03 ± 0.03	49.56/20	>99.999
PKS 1442+101.....	1.70	$1.9^{+1.2}_{-0.9}$	0.46 ± 0.35	23.2/24	
		1.70 fixed	0.41 ± 0.10	23.4/23	...
S4 1745+624	3.31	$6.8^{+0.30}_{-3.0}$	$0.78^{+1.0}_{-0.44}$	14.5/16	
		3.31 fixed	0.26 ± 0.13	19.1/17	96.8

observation are then needed to assess the nature of this source. MS 03363−2546 is not detected in radio by Stocke et al. (1992). The limit on the radio flux ensures that this quasar is a truly radio-quiet source. The origin of the cutoffs of MS 03363−2546 and US 3333 is unknown and deserves follow-up studies. The probability of finding by chance the detected number of cutoff radio-quiet quasars at $z < 2.2$, assuming a frequency of cutoffs similar to that of radio-loud quasars, is 1.3%.

6. COMPARISON WITH PREVIOUS RESULTS

Results on the *ROSAT* pointed observations of the quasars in Table 3 have been published by Elvis et al. (1994b; PKS 0438−436, PKS 2126−158, S4 0636+680), Elvis et al. (1994a; 3C 212), Maraschi et al. (1995; PKS 1334−127), Brunner et al. (1994, 4C 71.07), Buhler et al. (1995; PKS 0537−286), Bechtold et al. (1994; PKS 1442+101 and S4 1745+624).

The spectral fitting results in Table 6 generally agree well with the results presented in the above papers. Maraschi et al. (1995) use a Galactic N_H higher than the one we adopted (from Stark et al. 1992) by about 1.6×10^{20} cm^{-2}, and as a result conclude that there is little evidence for absorption in this source.

Some of the quasars in Table 3 have also been observed by *ASCA*; see Siebert et al. (1996; PKS 0537−286), Cappi et al. (1997; PKS 0438−436, PKS 0537−286, 4C 71.07, PKS 2126−158). The results found by these authors are consistent with those obtained from the *ROSAT* observations, with the exception of 4C 71.07, for which Cappi et al. (1997) report significant intrinsic absorption (of about 8×10^{20} cm^{-2}). The comparison between the *ROSAT* and *ASCA* data implies a variation in the absorber column density on a timescale of less than 2.6 yr in this source.

Cappi et al. (1997) discuss in detail the possibility that low-energy absorption in addition to the 21 cm value in their sample of high-redshift quasars may be due to molecular gas. For the four quasars in common between their and our sample, they find no strong evidence for Galactic molecular gas absorption. We note here that our limit on the Galactic (21 cm) N_H effectively excludes low Galactic latitude sources from our sample, thus minimizing the probability for contamination from Galactic molecular clouds, which are strongly concentrated toward the Galactic plane. The CO survey by Blitz, Magnani, & Mundy (1984) finds that molecular gas is uncommon at high Galactic latitudes. The only quasar known to be affected by molecular gas absorption (NRAO 140; Marscher 1988, Turner et al. 1995) lies at low Galactic latitude and was excluded from our sample because it has a Galactic (21 cm) N_H of 1.4×10^{21} cm^{-2}. Furthermore, de Vries, Heithausen, & Thaddeus (1987) found that high Galactic latitude molecular clouds differ from the Galactic plane clouds, so that their CO-to-H_2 conversion factor is significantly smaller: $\sim 0.5 \times 1020$

instead of $\sim(2\text{–}4) \times 1020$ molecules cm^{-2} $(K^{-1}\ km^{-1}\ s)^{-1}$ (Combes 1991). This would reduce the additional hydrogen column density implied by any CO emission by a factor of ~ 6.

The evolution of the quasar X-ray spectrum has also been studied by three groups: Schartel et al. (1996a), who used a sample drawn from the RASS containing all quasars with $M_V < -23$ and more than 80 RASS counts; Schartel et al. (1996b) used the large bright quasar sample (LBQS) quasars observed during the RASS (using both detections and nondetections); Puchnarewicz et al. (1996) used active galactic nuclei (AGNs) identified in the *ROSAT* International X-Ray/Optical Survey (RIXOS).

All the radio-quiet objects in Schartel et al. (1996a) are at $z < 0.5$, while radio-loud objects are detected up to $z = 2.5$. The indices of the radio-quiet objects are fully consistent with those of the WGACAT quasars. The PSPC spectral indices of radio-loud objects show a significant flattening above $z \sim 1$, which is interpreted by Schartel et al. in terms of a selection effect and/or a redshift effect, if quasar spectra are not simple power laws (but rather have a concave shape). In the WGACAT quasars we see little change in either α_S or α_H in the range $0.1 < z < 2$, most of the evolution being confined to redshifts higher than ~ 2.

On the other hand, most of the LBQS objects studied by Schartel et al. (1996b) are radio-quiet quasars. Schartel et al. (1996b) find marginal ($2\ \sigma$) evidence for a flattening of LBQS spectra at $z \gtrsim 1.5$. This result is consistent with our findings (see § 3.3.2 above) based on WGACAT quasars. In particular, the slopes reported by Schartel et al. (1996b) agree well with those in Table 1. Again, the study of the evolution of the spectrum of radio-quiet quasars is limited by the fact that high-redshift radio-quiet quasars are faint and not easy to observe with *ROSAT*.

Puchnarewicz et al. (1996) find a mean energy index significantly flatter than those obtained from the WGACAT quasars. They also find no evidence for a change in α_X with z. The flat average slope reported by Puchnarewicz et al. could be due to the selection criteria used to define the sample (a flux limit of 3×10^{-14} ergs cm^{-2} s^{-1} in the *ROSAT* 0.4–2 keV "hard band"), which favors the inclusion in the sample of flatter AGNs. Furthermore, the correlation of the optical–to–X-ray index with the X-ray spectral index (like the one found in Seyfert galaxies and low-redshift quasars; see, e.g., Walter & Fink 1993 and Fiore et al. 1995) can select preferentially flat X-ray quasars when considering a strictly X-ray–selected sample (low optical–to–X-ray index). We also note (from their Fig. 3) that in their sample there are a few quasars with a very flat spectral index, possibly due to absorption, which tend to lower the average index. These quasars have a red optical continuum, strengthening the evidence for absorption in these cases.

Also, the fraction of radio-loud AGNs in the RIXOS is unknown. The energy index Puchnarewicz et al. (1996) find at $2 < z < 3$ is similar to the index we find in the same redshift interval for radio-loud objects. At low redshift the radio-quiet population should dominate in number (because of its much larger volume density). However, we note that a similar X-ray flux-limited survey (Schartel et al. 1996a) is completely dominated by radio-loud objects at $z \gtrsim 0.5$, since radio-loud objects are brighter in X-rays than radio-quiet ones (e.g., Zamorani et al. 1981; Green et al. 1995). Therefore, the RIXOS indices, at least at high redshift, could be dominated by the radio-loud population.

7. CONCLUSIONS

We have studied the two-color X-ray spectra of a sample of about 167 radio-loud quasars and 286 "bona fide" radio-quiet quasars. Radio-loud quasars cover the whole redshift space from 0.1 to 4 rather uniformly, while there are only three radio-quiet quasars at $z > 2.5$ as against 12 radio-loud quasars at the same redshifts. Any conclusion on radio-quiet quasars then applies to $z \lesssim 2$ only.

Concerning the low-energy cutoff we have established the following:

1. Low-energy X-ray cutoffs are more commonly (and perhaps exclusively) associated with radio-loud quasars. Detailed spectral fits allow us to add, with some confidence, that photoelectric absorption is a likely origin of the "low-energy cutoffs." The conclusion is that *low-energy X-ray cutoffs are associated with the quasars*, and not with intervening systems, since those would affect radio-quiet and radio-loud quasars equally.

2. Among radio-loud quasars, those at high redshift have a lower mean α_S than those at low z ($P = 0.04\%$), with many lying in the X-ray cutoff zone. Detailed spectral analysis of all candidate cutoff quasars show four robust cutoff detections at redshift higher than 2.2. The probability that the fraction of cutoff quasars among the 18 objects at $z > 2.2$ is similar to that of radio-loud quasars at $z < 2.2$ is very small, about 0.002% (using the binomial distribution). This indicates that cutoffs were more common in the past than they are now. That is, *the X-ray cutoffs show evolution with cosmic epoch.*

3. The degeneracy between redshift and luminosity found in flux-limited samples of quasars was tested by using a partial correlation analysis. We found that while α_S is truly anticorrelated with redshift at the 99.9% confidence level, in the case of α_H the observed anticorrelation with redshift is mostly due to a strong dependence on luminosity. Therefore, the cutoffs are an evolutionary, not a luminosity, effect.

Concerning the emitted X-ray spectra of quasars, we have established the following:

4. The distribution of α_S of radio-quiet quasars is consistent with that of α_H for $z \lesssim 2$. This uniformity suggests a single emission mechanism dominating the whole *ROSAT* band (cf. Laor et al. 1997) up to a redshift of about 2. We find marginal evidence for a flattening of α_H ($P = 4.5\%$) going from $z < 1$ to $z = 2$, in agreement with previous studies (Schartel et al. 1996b). This can be due to a selection effect even if quasar X-ray spectra are simple power laws, because at high redshift the steepest (and therefore faintest) sources would not be detected. However, it is well known that *ROSAT* PSPC 0.1–2 keV spectral indices of Seyfert 1 galaxies and low-redshift radio-quiet quasars are much steeper than those observed above 2 keV (e.g., Walter & Fink 1993; Fiore et al. 1994; Laor et al. 1997). If the spectrum of these AGNs is made up of two distinct components that are equal at a typical energy E_0, the flattening of α_H at $z > 1$ would suggest that E_0 lies in the range 2–4 keV (quasar frame).

5. Radio-loud quasars at $z < 2.2$ show a "concave" spectrum ($\alpha_H < \alpha_S$ by ~ 0.2). Both indices are much flatter than those of radio-quiet quasars. This new result is in line with the suggestion of Wilkes & Elvis (1987) that the X-ray spectrum of radio-loud quasars may be due to an additional component beyond those seen in radio-quiet quasars.

However, it may also imply different processes at work in radio-loud and radio-quiet sources (as recently suggested by Laor et al. 1997). At $z \gtrsim 2$, the average soft and hard indices are similar and both significantly smaller than at lower redshifts. This could be due to the soft component of radio-loud quasars being completely shifted out of the PSPC band at $z > 2$. Most $z > 2$ radio-loud quasars in our sample have flat radio spectra. Padovani et al. (1997) suggested that these quasars are analogs to LBL BL Lac objects, that is, BL Lac objects with maximum energy emission in the IR-optical band. Their high-energy radiation should then be dominated by inverse Compton emission. At $z > 2$ we are then likely seeing pure inverse Compton emission. At lower redshift the *ROSAT* PSPC band could sample a mixture of inverse Compton emission, the tail of the synchrotron component peaking in the infrared and thermal emission from the hypothesized accretion disk.

The radio and optical properties of the quasars with low energy X-ray cutoffs will be discussed in more detail in a companion paper (Elvis et al. 1998a [Paper II]).

This research has made use of the BROWSE program developed by the ESA/*EXOSAT* Observatory, NASA/HEASARC, and the NASA/IPAC Extragalactic Database (NED), which is operated by the Jet Propulsion Laboratory, California Institute of Technology, under contract with the National Aeronautics and Space Administration.

REFERENCES

Anders, E., & Ebihara, M. 1982, Geochim. Cosmochim. Acta, 46, 2363
Bechtold, J., et al. 1994, AJ, 108, 374
Blitz, L., Magnani, K., & Mundy, L. 1984, ApJ, 282, L9
Brunner, H., Lamer, G., Worrall, D., & Staubert, R. 1994, A&A, 287, 436
Buhler, P., Courvoisier, T. J.-L., Staubert, R., Brunner, H., & Lamer, G. 1995, A&A, 295, 309
Cappi, M., et al. 1997, ApJ, in press
Ciliegi, P., Elvis, M., Wilkes, B. J., Boyle, B. J., McMahon, R. G., & Maccacaro, T. 1995, MNRAS, 277, 1463
Ciliegi, P., & Maccacaro, T. 1996, MNRAS, 282, 477
Combes, F. 1991, ARA&A, 29, 195
Condon, J. J., Cotton, W. D., Greisen, E. W., Yin, Q. F., Perley, R. A., Taylor, G. B., & Broderick, J. J. 1998, http://www.cv.nrao.edu/~jcondon/nvss.html
Dalla Casa, D., Fanti, C., Schilizzi, R. T., & Spencer, R. E. 1995, A&A, 295, 27
de Vries, H. W., Heithausen, A., & Thaddeus, P. 1987, ApJ, 319, 723
Elvis, M., Fiore, F., Giommi, P., & Padovani, P. 1998a, ApJ, 492, 91 (Paper II)
———. 1998b, MNRAS, in press
Elvis, M., Fiore, F., Mathur, S., & Wilkes, B. 1994a, ApJ, 425, 103
Elvis, M., Fiore, F., Wilkes, B. J., McDowell, J., & Bechtold, J. 1994b, ApJ, 422, 60
Elvis, M., & Lawrence, A. 1985, in Astrophysics of Active Galaxies and Quasi-stellar Objects, ed. J. Miller (Mill Valley: University Science Books)
Elvis, M., Mathur, S., & Wilkes, B. 1995, ApJ, 452, 230
Fiore, F., Elvis, M., McDowell, J. C., Siemiginowska, A., & Wilkes, B. J. 1994, ApJ, 431, 515
Fiore, F., Elvis, M., Siemiginowska, A., Wilkes, B. J., McDowell, J. C., & Mathur, S. 1995, ApJ, 449, 74
Giommi, P., et al. 1998, in preparation
Green, P. J., et al. 1995, ApJ, 450, 51
Hasinger, G., et al. 1992, Legacy, 2, 77, OGIP MEMO, CAL/ROS/92-001
Heiles, C., & Cleary, M. N. 1979, Australian J. Phys. Suppl., 47, 1
Hewitt, A., & Burbidge, G. 1993, ApJS, 87, 451
Kellermann, K. I., Sramek, R., Schmidt, M., Shaffer, D. B., & Green, R. 1989, AJ, 98, 1195
Kendall, M., & Stuart, A. 1979, The Advanced Theory of Statistics (New York: Macmillan)
Laor, A., Fiore, F., Elvis, M., Wilkes, B. J., & McDowell, J. C. M. 1994, ApJ, 435, 611
Laor, A., Fiore, F., Elvis, M., Wilkes, B. J., & McDowell, J. C. M. 1997, ApJ, 477, 93
Lawrence, A., & Elvis, M. 1982, ApJ, 256 410
Maraschi, L., Fossati, G., Tagliaferri, G., & Treves, A. 1995, ApJ, 443, 478
Marscher, A. 1988, ApJ, 334, 552
Morrison, R., & McCammon, D. 1983, ApJ, 270, 119
Nicastro, F., et al. 1997, ApJ, in preparation
Padovani, P., & Giommi, P. 1996, MNRAS, 279, 526
Padovani, P., Giommi, P., & Fiore, F. 1997, MNRAS, 284, 569
Puchnarewicz, E. M., et al. 1996, MNRAS, 281, 1243
Schartel, N., Walter, R., Fink, H. H., & Trümper, J. 1996a, A&A, 307, 33
Schartel, N., et al. 1996b, MNRAS, 283, 101
Siebert, J., Matsuoka, M., Brinkmann, W., Cappi, M., Mihara, T., & Takahashi, T. 1996, A&A, 307, 8
Siegel, S. 1956, Nonparametric Statistics (New York: McGraw-Hill)
Snowden, S. L., McCammon, D., Burrows, D. N., & Mendenhall, J. A. 1994, ApJ, 424 714
Snowden, S. L., Plucinsky, P. P., Briel, U., Hasinger, G., & Pfefferman, E. 1992, ApJ, 393, 819
Snowden, S. L., et al. 1995, ApJ, 454, 643
———. 1997, ApJ, 485, in press
Stark, A. A., Gammie, C. F., Wilson, R. W., Bally, J., Linke, R. A., Heiles, C., & Hurwitz, M. 1992, ApJS, 77
Stickel, M., & Kühr, H. 1994, A&AS, 103, 349
Stickel, M., Meisenheimer, K., & Kühr, H. 1994, A&AS, 105, 211
Stocke, J. T., Morris, S. L., Weymann, R. J., & Foltz, C. B. 1992, ApJ, 396, 487
Turner, T. J., et al. 1995, ApJ, 445, 660
Véron-Cetty, M.-P., & Véron, P. 1993, A Catalogue of Quasars and Active Nuclei (6th ed.; ESO Sci. Rep. 13)
von Montigny, C., et al. 1995, ApJ, 440, 525
Voges, W., et al. 1994, ROSATSRC, announcement at *ROSAT* Workshop, on behalf of the *ROSAT* Consortium
Walter, R., & Fink, H. H. 1993, A&A, 274, 105
White, N. E., Giommi, P., & Angelini, L. 1995, http://heasarc.gsfc.nasa.gov/W3Browse/all/wgacat.html
Wilkes, B. J., & Elvis, M. 1987, ApJ, 323, 243
Wilkes, B. J., Elvis, M., Fiore, F., McDowell, J. C., Tananbaum, H., & Lawrence, A. 1992, ApJ, 393, L1
Zamorani, G., et al. 1981, ApJ, 245, 357